ELSEVIER

www.elsevier.nl/locate/jelechem

Journal of Electroanalytical Chemistry 491 (2000) 95–102

Journal of Electroanalytical Chemistry

Chronocoulometric studies of chloride adsorption at the Pt(111) electrode surface

Nanhai Li, Jacek Lipkowski *

Guelph-Waterloo Center for Graduate Work in Chemistry, Guelph Campus, Department of Chemistry and Biochemistry, University of Guelph, Guelph, Ont., Canada N1G 2W 1

Received 20 January 2000; received in revised form 22 May 2000; accepted 27 May 2000

Dedicated to Professor E. Gileadi on the occasion of his retirement from the University of Tel Aviv and in recognition of his contribution to electrochemistry

Abstract

Chronocoulometry and a thermodynamic analysis of charge density data were used to describe chloride adsorption at the Pt(111) electrode surface. The Gibbs excess, the Gibbs energy of adsorption, the number of electrons flowing to the interface per adsorbed chloride ion at a constant potential (electrosorption valency) and at constant chloride concentration (reciprocal of the Esin–Markov coefficient) were determined. Chloride forms a chemisorption bond with platinum. The charge numbers at constant potential and at constant chloride concentration are close to unity. This result suggests that the polarity of the chemisorption bond is very small. The highest packing density of chloride determined by the thermodynamic method corresponds to 0.43 ML. This number agrees well with coverage determined in recent surface X-ray scattering experiments [1]. Adsorption of chloride at Pt(111) is potential and pH dependent. We have demonstrated that at negative potentials, co-adsorption of Cl and hydrogen atoms has a synergistic character. In contrast the adsorption of chloride and OH at positive potentials has a competitive nature.

Keywords: Chloride adsorption; Pt(111) electrode; Capacitive chronocoulometry

1. Introduction

The objective of this project is to describe thermodynamics of chloride adsorption at the Pt(111) electrode using charge density data determined with the help of the chronocoulometric technique. Chloride adsorption at the Pt(111) electrode has been recently investigated by an in situ surface scattering technique [1] and by the CO displacement method [2]. Adsorption of Cl^- at the Pt(111) electrode has also been investigated by a combination of cyclic voltammetry and ex situ techniques such as Auger electron spectroscopy (AES) and low energy electron diffraction (LEED) [3,4]. There is a significant amount of information concerning adsorption of chlorine [5–7] and HCl [8] or $MgCl_2$ [9] at the Pt single crystal surfaces under UHV conditions. In addition there are earlier studies of chloride adsorption at polycrystalline Pt using either radiotracers [10], depletion of the bulk concentration [11] or electrochemical methods [12–14]. Molecular dynamics calculations have also been applied to simulate adsorption of Cl^- at the charged water | platinum interface [15]. Anions are known to influence the metal underpotential deposition (upd) reaction [16] and there is a rich literature that describes the effect of chloride on upd phenomena at the Pt single crystal surfaces [17–26].

Despite these extensive efforts, reproducible surface concentration data for chloride adsorption at Pt were measured only for large area, platinized–platinum electrodes [10,11]. For the smooth Pt(111) single crystal surface, earlier ex situ AES measurements gave significantly lower chloride coverages [3,18] than the most recent estimate based on in situ SXS experiments [1]. Recently, we employed chronocoulometry and the thermodynamic analysis of the charge density data to deter-

* Corresponding author. Fax: +1-519-7661499.
E-mail address: lipkowski@chembio.uoguelph.ca (J. Lipkowski).

0022-0728/00/$ - see front matter
PII: S0022-0728(00)00199-6

mine the surface concentration of bisulfate at the Pt(111) electrode surface [27]. In the present work we have used this method to determine surface concentrations of chloride adsorbed at the Pt(111) electrode surface. In addition, the present work has provided thermodynamic data such as Gibbs energies of adsorption and charge numbers per adsorbed chloride ion at constant electrode potential and at constant chloride concentration in the bulk.

2. Experimental

All measurements were carried out in a three-electrode glass cell. A Pt single crystal bead was cut along the (111) orientation (geometric area of the (111) surface 0.043 cm^2). The electrode was annealed in a hydrogen + air flame and then cooled down in a hydrogen atmosphere and later quenched with ultrapure water, before each experiment [28]. Cyclic voltammetry was used to check the cleanliness of the electrode. The counter electrode was a platinum coil cleaned by flame annealing. All the electrode potentials were measured with respect to the saturated calomel electrode (SCE) reference electrode. SCE was connected to the electrolyte through a salt bridge (saturated KCl solution).

Water was purified in a tandem of a MilliQ and a Milli-Q plus UV system (18.2 MΩ resistivity). The support electrolyte was 0.1 M $KClO_4$. The pH of the solution was adjusted to 3 by the addition of $HClO_4$. Potassium perchlorate was purified as described in Ref. [29]. Perchloric acid (Seastar Chemicals) and potassium chloride (Aldrich Chemical Company, Inc., 99.98%) were used without further purification. The solution was purged with argon to remove oxygen. The electrochemical experiments were performed using a PAR model 173 potentiostat controlled by a computer. The data were acquired via a plug-in acquisition board (RC Electronics model IS-16). Custom software was used to record cyclic voltammograms (CVs) and to perform the chronocoulometric experiments. All experiments were conducted at room temperature (20 ± 2°C).

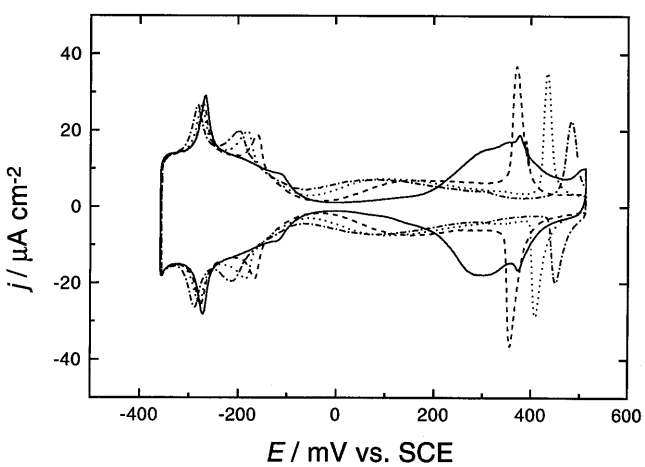

Fig. 1. Cyclic voltammograms recorded in 0.1 M $KClO_4 + 10^{-3}$ M $HClO_4 + x$M KCl: solid line, $x = 0$; dashed line, $x = 1 \times 10^{-4}$; dotted line, $x = 1 \times 10^{-3}$; dashed and dotted line, $x = 5 \times 10^{-3}$.

3. Results and discussion

3.1. Data acquisition

The species that may be adsorbed at the Pt electrode surface from the mixed perchlorate–chloride electrolyte are hydrogen atoms H_{ad}, chloride ions Cl^-_{ad}, perchlorate ions ClO_4^- and, at sufficiently positive potentials, a product of a partial oxidation of water OH_{ad}. Consequently, at negative potentials the adsorption of chloride ions takes place concomitantly with the adsorption of hydrogen adatoms and at more positive potentials with the adsorption of OH_{ad}. The adsorption of Cl^- has a competitive character and depends on pH [3]. The thermodynamic method used here to determine the surface concentration of adsorbed chloride relies on the so-called back integration of the charge–potential curves [27]. The back integration procedure requires that, for the whole series of KCl concentrations investigated, chloride ions are totally desorbed from the electrode surface at sufficiently negative potentials. Cyclic voltammetry was initially employed to characterize chloride adsorption at the Pt(111) electrode surface qualitatively and to find the best experimental conditions for further quantitative studies. We have found that the best conditions for chronocoulometric experiments are at pH ~ 3. In solutions of lower pH, the hydrogen evolution reaction overlaps with desorption of chloride ions and in solutions of higher pH, adsorption of OH_{ad} restricts the potential range within which chloride adsorption may be investigated.

Fig. 1 shows the CV curves recorded in 0.10 M $KClO_4 + 10^{-3}$ M $HClO_4$ electrolyte without and with the presence of chloride ions. The CV recorded in the pure electrolyte displays a characteristic 'butterfly' shape. The peaks at 375 mV are less sharp and somewhat less reversible in the solution of pH 3 than in solutions with higher proton concentration. The shape of the CV changes significantly in the presence of chloride ion. The voltammograms recorded for different KCl solutions display similar fingerprints to that reported by Stern et al. [3] in solutions of pH ~ 4. Chloride adsorption apparently overlaps with the adsorption of hydrogen. However, at sufficiently negative potentials ($E < -320$ mV) voltammetric currents recorded in the presence of Cl^- merge with the current recorded for the chloride free solution. This behavior indicates that chloride ions are totally desorbed from the electrode surface at these negative potentials. High

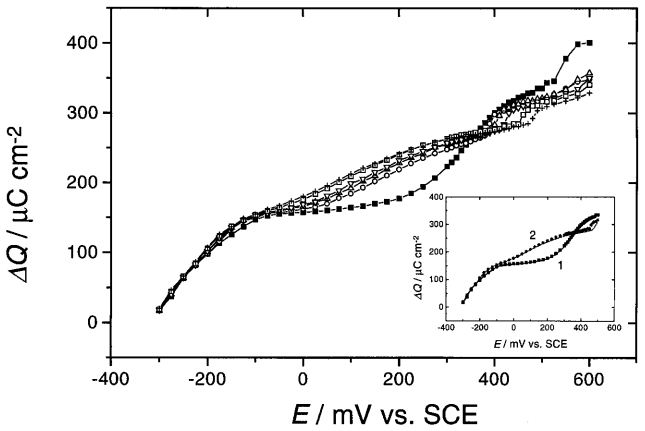

Fig. 2. The difference between the total charge density at potential E and base potential $E_{base} = -0.325$ V plotted against the electrode potential E for 0.1 M $KClO_4 + 10^{-3}$ M $HClO_4 + x$M KCl solutions with x equal to: 0 (■), 1×10^{-4} (○), 5×10^{-4} (△), 1×10^{-3} (▽), 5×10^{-3} (□), 1×10^{-2} (+). The inset shows the comparison of charge densities determined from the potential step experiments (experimental points) and by integration of CVs (solid line) for 0.1 M $KClO_4 + 10^{-3}$ M $HClO_4 + x$M KCl solution with: curve 1, $x = 0$; curve 2, $x = 1 \times 10^{-2}$ M KCl.

reversible or quasi-reversible peaks seen in the potential range 350–450 mV were assigned by Stern et al. [3] to the adsorption of oxygen species such as OH_{ad}. These peaks move in the positive direction when the bulk chloride concentration increases, indicating that the adsorption of chloride and the oxygen species has a competitive character.

The potential step experiments and the procedure described in Ref. [27] were used for quantitative data acquisition. The potential was held at $E > E_{base} = -325$ mV for a period of 30 s, which was sufficiently long to allow the adsorption equilibrium to be established for the chloride and hydronium ion concentrations used in this study. Then the potential was stepped to E_{base} and the transient current due to the desorption of Cl^- and adsorption of hydrogen adatoms was recorded within a time window of 400 ms. This current was then integrated to give the charge density difference ΔQ between the total charge densities at potentials E and E_{ads}. The charge density difference includes the contributions from recharging of the double layer, the desorption of chloride, perchlorate and OH from the electrode surface and the adsorption of hydrogen on the surface. This procedure was repeated for E covering the potential range from -300 to 600 mV using 25 mV increments between each step. The ΔQ versus potential curves were determined for 14 electrolyte solutions of the composition 0.1 M $KClO_4 + 10^{-3}$ M $HClO_4 + x$M KCl where x varied from 1.0×10^{-4} to 10^{-2}. For selected solutions, the total charge densities are plotted versus the electrode potential in Fig. 2. The shape of the charge density curves is consistent with the shape of cyclic voltammetry curves. The positions of the inflection points on the ΔQ curves correlate well with the position of peaks on CVs. The inset to Fig. 2 shows that for the chloride free and for 10^{-2} M chloride solutions, the charge density curves determined by chronocoulometry agree well with the charge densities determined by integration of the cyclic voltammograms. However, small differences are seen for the charge density curves in 10^{-2} M chloride solution at $E > 450$ mV. They reflect the fact that the voltammetric peaks due to the adsorption of the oxygen species become slightly irreversible in solutions with higher chloride concentration. The charge density curves constitute the basic set of data from which the surface concentrations of chloride are determined using thermodynamics of the so-called perfectly polarized electrode introduced by Frumkin and Petrii [30].

3.2. Data analysis

3.2.1. Gibbs excess

The electrocapillary equation for the Pt | solution interface may be written as:

$$-\mathrm{d}\gamma = Q\,\mathrm{d}E + \Gamma_{Cl^-}\,\mathrm{d}\mu_{Cl^-} + \Gamma_{H^+}\,\mathrm{d}\mu_{H^+} + \Gamma_{OH^-}\,\mathrm{d}\mu_{OH^-} + \Gamma_{ClO_4^-}\,\mathrm{d}\mu_{ClO_4^-} + \Gamma_{K^+}\,\mathrm{d}\mu_{K^+} \quad (1)$$

where γ is the interfacial tension, Q is the total charge flowing to the metal side, E is the electrode potential, Γ is the Gibbs excess of the adsorbed species and μ is the chemical potential. For experiments performed in solutions of a constant ionic strength and a constant $HClO_4$ concentration, Eq. (1) can be simplified to the following form:

$$-\mathrm{d}\gamma = Q\,\mathrm{d}E + \Gamma_{Cl^-}\,\mathrm{d}\mu_{KCl} = Q\,\mathrm{d}E + \Gamma_{Cl^-}RT\ln c_{KCl} \quad (2)$$

where c_{KCl} is the concentration of KCl. The potential of zero total charge (pzc) of the Pt(111) electrode is unknown and hence we were not able to determine the absolute values of Q. However, the ΔQ values were measured in a sufficiently broad range of potentials that encompassed E where chloride is desorbed from the electrode surface. Therefore ΔQ could be used to calculate surface pressure $\pi = \gamma_{\Theta=0} - \gamma_\Theta$ by employing the back integration procedure described in [27]:

$$\pi = \gamma_{\Theta=0} - \gamma_\Theta = \int_{E_1}^{E_2} (\Delta Q_\Theta - \Delta Q_{\Theta=0})\mathrm{d}E \quad (3)$$

where $\gamma_{\Theta=0}$, $\Delta Q_{\Theta=0}$ and γ_Θ, ΔQ_Θ denote the surface tension and the charge density measured in the absence and presence of Cl^- respectively.

The Gibbs excess of chloride may be then calculated by differentiation of the surface pressure with respect to the logarithm of the bulk chloride concentration using the formula:

$$\Gamma_{Cl^-} = \frac{1}{RT}\left[\frac{\partial \pi}{\partial \ln c_{KCl}}\right]_{E,\mu_{HClO_4}} \quad (4)$$

Fig. 3 shows the surface pressure versus potential plots determined by the back integration of the charge density curves, for selected chloride solutions. The curves display a maximum at potentials close to 350 mV, where the charge density curves determined in the presence of chloride intersect the charge density curve for the chloride free supporting electrolyte. This is the potential of maximum adsorption at which the Gibbs excess values will also display a maximum.

At constant potential, the surface pressures were plotted against $\ln c_{KCl}$ and differentiated to determine the Gibbs excess of the adsorbed chloride. Fig. 4 shows the calculated Γ_{Cl^-} versus E plots. In principle these values represent the total Gibbs excess, that is the Gibbs excess of chloride in both the inner and diffuse part of the double layer. However, in the presence of a tenfold (or more) excess of a supporting electrolyte the excess of chloride in the diffuse layer may be considered as negligible and the measured Gibbs excess as equal to the concentration of specifically (contact) adsorbed chloride ion.

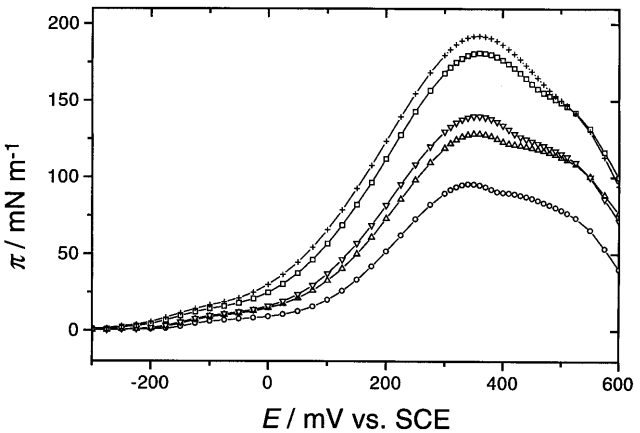

Fig. 3. Surface pressure π plotted against electrode potential for chloride adsorption at Pt(111) surface from 0.1 M $KClO_4 + 10^{-3}$ M $HClO_4 + x$M KCl solutions with x equal to: 1×10^{-4} (○), 5×10^{-4} (△), 1×10^{-3} (▽), 5×10^{-3} (□), 1×10^{-2} (+).

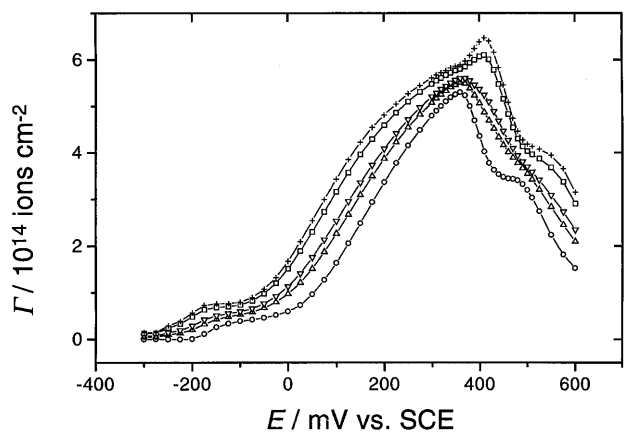

Fig. 4. The Gibbs excess of chloride adsorbed from 0.1 M $KClO_4 + 10^{-3}$ M $HClO_4 + x$M KCl solutions with x equal to: 1×10^{-4} (○), 5×10^{-4} (△), 1×10^{-3} (▽), 5×10^{-3} (□), 1×10^{-2} (+).

The Γ_{Cl^-} versus E plots display a number of steps and inflections indicating that the character of Cl^- adsorption changes with the electrode potential. The first small step is observed at $E < 0$ V where the coverage of the electrode surface by chloride ions is less than 0.1 ML (one monolayer (ML) corresponds to the Pt atom density at the ideal (111) surface equal to 1.5×10^{15} atom cm^{-2}). This is the potential region where hydrogen atoms are adsorbed at the Pt electrode surface and chloride ions are co-adsorbed with hydrogen adatoms. The section for $0 < E < 0.35$ V (SCE), where the surface concentration of Cl^- rises steeply, corresponds to the so called 'double layer' region where in principle neither H_{ad} nor OH_{ad} are present at the electrode surface. The surface concentration of Cl^- decreases with potential when $E > 0.35$ V. These potentials are more positive than the values of E corresponding to the position of sharp reversible peaks on CVs assigned by Stern et al. [3] to the onset of oxygen species adsorption. Apparently, chloride ions are displaced from the electrode surface by OH_{ad}, at these positive potentials.

For the Pt(111) electrode, the surface concentrations of Cl^- determined by the chronocoulometric method are significantly higher than the coverages determined earlier using ex situ AES [3,18]. They are also higher than the coverages measured for a platinized Pt electrode [10,11] using either radiotracer or bulk chloride depletion methods. However, the results presented in Fig. 4 agree very well with chloride coverages determined recently using the in situ SXS technique [1]. In Fig. 4, for 10^{-2} M chloride solution, the maximum surface concentration of Cl^- amounts to about 6.5×10^{14} ions cm^{-2}. This number density corresponds to 0.43 ML, while the results reported in Ref. [1] show that at $E = 0.4$ V chloride coverage should be between 0.4 to 0.5 ML in 0.1 M $HClO_4 + 0.01$ M KCl solution.

3.2.2. Gibbs energy of adsorption

To determine the Gibbs energies of adsorption we applied the so-called 'square root' isotherm suggested by Parsons and co-workers [31,32]:

$$\ln(kTc_{KCl}) + \ln \beta = \ln \pi + B\pi^{1/2} \quad (5)$$

where $\beta = \exp(-\Delta G/kT)$ is the adsorption equilibrium constant, ΔG is the Gibbs energy of adsorption, β is a constant and π is the surface pressure. The square-root isotherm is an empirical isotherm and should be viewed as a convenient procedure to linearize experimental data only. Fig. 5 shows plots of the square root of the surface pressure versus $\ln(kTc_{KCl}/\pi)$ at constant potential. The plots are nearly linear and when fitted to a

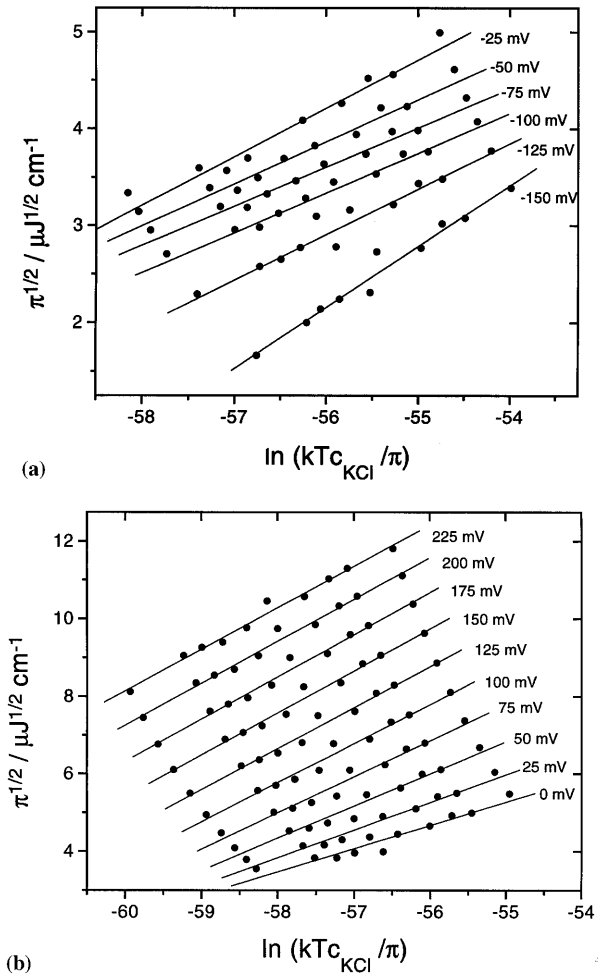

Fig. 5. Fit of the adsorption data to the square root isotherm (Eq. (5)) at constant electrode potential E indicated in Fig. 3: (a) $E<0$ mV; (b) $E\geq 0$ mV vs. SCE.

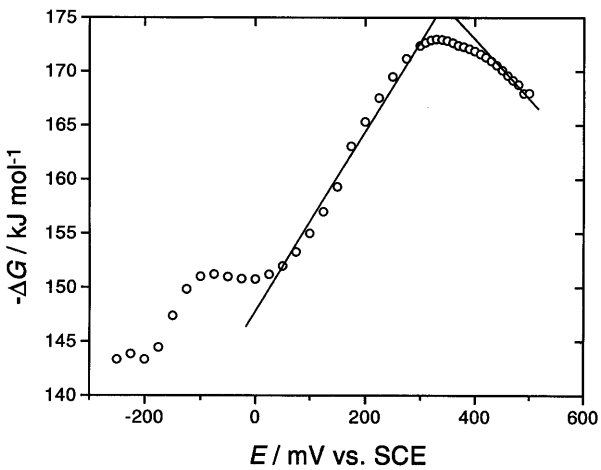

Fig. 6. Plot of the Gibbs energy of chloride adsorption at Pt(111) vs. electrode potential. The straight lines were drawn to determine the average slopes of the Gibbs energy plots for potential regions $0<E<300$ mV and $E>400$ mV, respectively.

linear regression give an intercept with $\ln(kTc_{\mathrm{KCl}}/\pi)$ at zero film pressure equal to:

$$\lim_{\pi=o}[\ln(kTc_{\mathrm{KCl}}/\pi)] = -\ln\beta = \Delta G/kT \tag{6}$$

from which the Gibbs energy of adsorption can be calculated. The Gibbs energies of adsorption determined using this procedure are plotted against the electrode potential in Fig. 6. The standard state is an 'ideal' $\Gamma = 1$ ion cm^{-2} for the adsorbed species and an 'ideal' $c_{\mathrm{KCl}} = 1$ mol dm^{-3} for the bulk species. In the potential range 0 to 300 mV the Gibbs energy change is approximately linear. It attains a minimum at about 350 mV which is the potential of maximum film pressure, and then it increases steeply. The increase of the Gibbs energy at positive potentials is apparently due to the displacement of adsorbed Cl^- by the adsorbed oxygen species.

3.2.3. Charge numbers per adsorbed chloride ion

The number of electrons flowing to the electrode surface per one specifically adsorbed ion at constant potential l, called frequently the 'electrosorption valency', may be determined from the derivative of the Gibbs energy with respect to the electrode potential. l can be calculated independently from the slope of the charge density versus Gibbs excess plots:

$$l = -\frac{1}{F}\left(\frac{\partial\Delta Q}{\partial\Gamma}\right)_E = \frac{1}{F}\left(\frac{\partial\Delta G}{\partial E}\right)_\Gamma \tag{7}$$

Thus the slope of the ΔQ versus Γ_{Cl^-} plot may be compared with the first derivative of the ΔG with respect to potential as a test of the reliability of the Gibbs energy data. Fig. 7 shows representative ΔQ versus Γ plots for selected electrode potentials. These plots are fairly linear and their slopes give l values that are plotted in Fig. 8. The charge number l apparently depends on potential. To explain this dependence, it is useful to express the measured change of the total charge ΔQ in terms of contributions from adsorbed chloride, hydrogen and oxygen species:

$$\Delta Q = \Delta Q_\infty - l_{\mathrm{Cl}^-}F\Delta\Gamma_{\mathrm{Cl}^-} - l_{\mathrm{H}^+}F\Delta\Gamma_{\mathrm{H}^+} - l_{\mathrm{OH}^-}F\Delta\Gamma_{\mathrm{OH}^-} \tag{8}$$

where l_i is the charge number per one adsorbed molecule of species i and ΔQ_∞ is the charge corresponding to charging of the so called infinite frequency capacity. Combining Eqs. (7) and (8), we can express the measured charge number l in terms of:

$$l = -\frac{1}{F}\left(\frac{\partial\Delta Q}{\partial\Gamma_{\mathrm{Cl}^-}}\right)_E = l_{\mathrm{Cl}^-} + l_{\mathrm{H}^+}\left(\frac{\partial\Gamma_{\mathrm{H}^+}}{\partial\Gamma_{\mathrm{Cl}^-}}\right)_E + l_{\mathrm{OH}^-}\left(\frac{\partial\Gamma_{\mathrm{OH}^-}}{\partial\Gamma_{\mathrm{Cl}^-}}\right)_E \tag{9}$$

The charge number $l \approx -1.0$ within the 'double layer' region corresponding to $50 < E < 300$ mV. Indepen-

dently, when a linear regression is applied to fit the segment of the ΔG versus E plot in this range of potentials (Fig. 6), the slope gives the value $l = -0.9$. Likewise, the slope of the line drawn in Fig. 6 through the ΔG values for $E > 400$ mV, corresponds to $l = -0.6$. Apparently, the charge numbers determined using the two independent routes are in reasonable agreement. This agreement indicates that no major errors were made in the calculation of the Gibbs energies and Gibbs excesses. These numbers are somewhat lower than the electrosorption valency reported for chloride ion to be around -1.2 by Orts et al. [2].

In the 'double layer' range, the derivatives of Γ_H and Γ_{OH} with respect to the surface chloride concentration are to a good approximation equal to zero and hence $l \approx l_{Cl^-}$. The charge number l_{Cl^-} may be used to calculate the surface dipole μ_s, which represents the dipole formed by an adsorbed anion and its image charge in the metal, using the formula [33,34]:

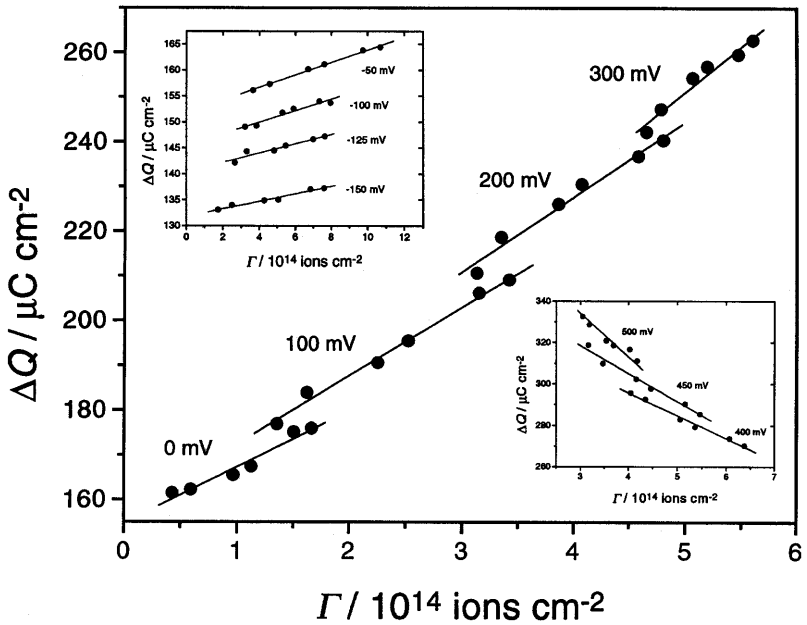

Fig. 7. Plots of the ΔQ vs. Γ_{Cl^-} plots taken at constant electrode potential values indicated in the Figure. The main section shows ΔQ vs. Γ_{Cl^-} plots for $0 \le E \le 300$ mV. The insets show the plots for $E < 0$ mV and $E > 300$ mV respectively.

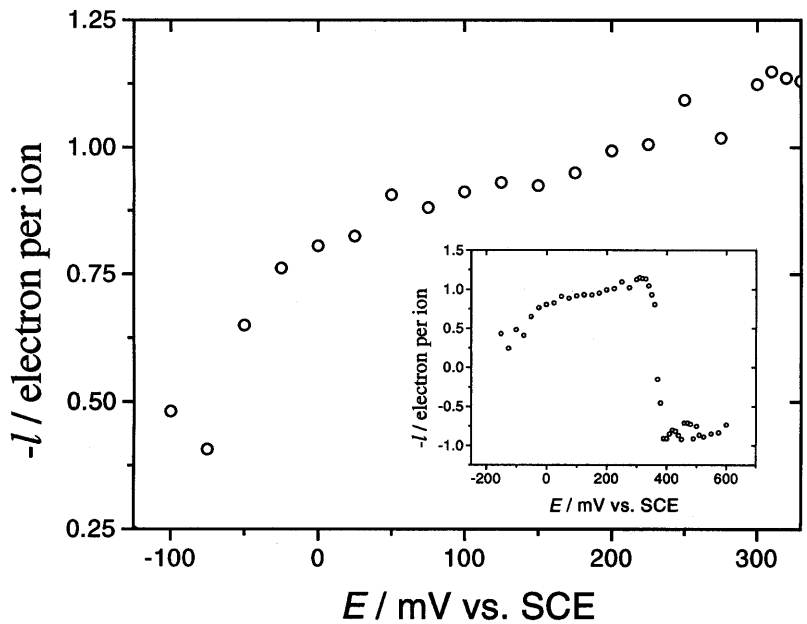

Fig. 8. Electrosorption valencies of chloride adsorption determined from the slope of the charge vs. Gibbs excess plots. Main section: $E < 300$ mV (SCE). Inset: the whole potential range.

$$\mu_s = \frac{z\varepsilon_o(1 - l/z)}{{}_QC} \quad (10)$$

where $z = -1$ is the charge of the chloride ion, ε_o is the permittivity of vacuum and ${}_QC$ is the capacity at the constant amount adsorbed. The surface dipole is a measure of the polarity of the electrosorption bond. In the present case, the value of $l_{Cl^-} \approx -1$ indicates that the surface dipole is close to zero. Apparently adsorption of Cl^- at Pt(111) is coupled with a significant redistribution of charge so that the adsorbed species may be considered as the chlorine atom.

At $E < 0$ the charge number l increases (the absolute value of l decreases). This is the potential region where hydrogen adsorption takes place and where $\Gamma_{OH} = 0$. Since $l_H = 1$ the observed change of l indicates that $\partial\Gamma_H/\partial\Gamma_{Cl^-} > 0$ and that adsorption of chloride and hydrogen adatoms have a co-operative character. The adsorption of chloride apparently promotes the adsorption of hydrogen. The first step seen on the Gibbs excess plots (Fig. 4) may therefore be assigned to a small enhancement of chloride adsorption by co-adsorbed hydrogen adatoms.

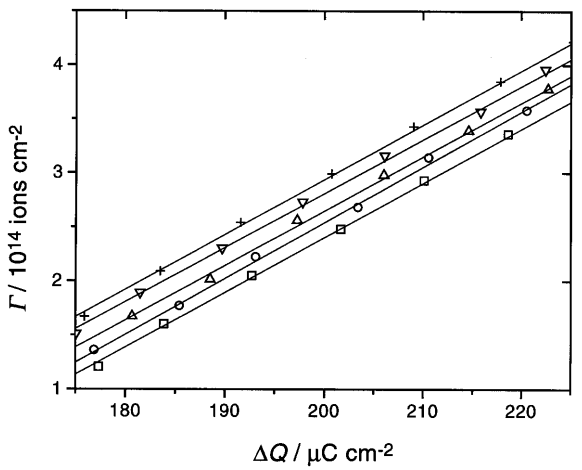

Fig. 9. Plots of the Gibbs excess of Cl^- against ΔQ for 0.1 M $KClO_4 + 10^{-3}$ M $HClO_4$ with the following KCl concentrations: 1×10^{-4} (□), 5×10^{-4} (○), 1×10^{-3} (△), 5×10^{-3} (▽), 1×10^{-2} (+) mol dm^{-3}.

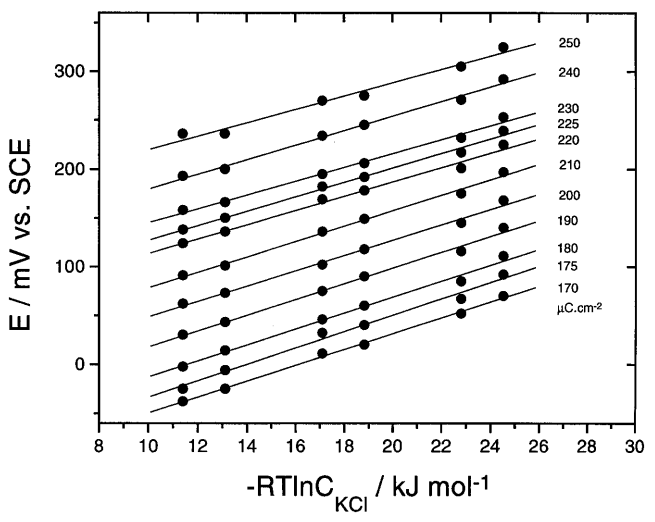

Fig. 10. Esin–Markov plots for selected ΔQ values indicated in the Figure.

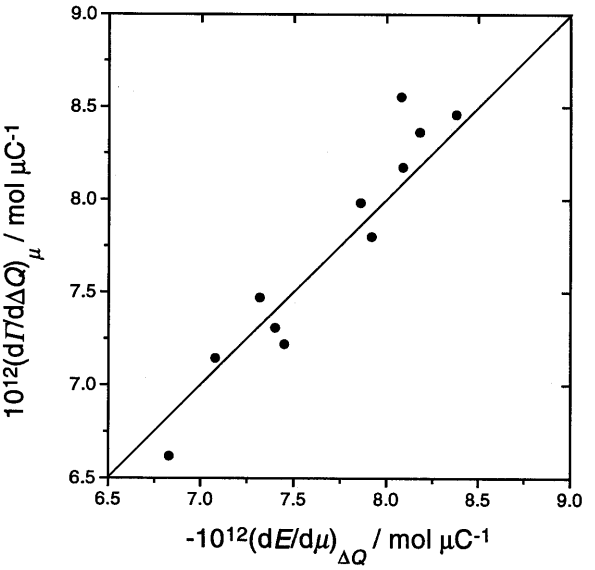

Fig. 11. Comparison of the Esin–Markov coefficients determined from the slope of the E vs. $\ln c_{KCl}$ plots and from the slope of the Γ_{Cl^-} vs. ΔQ relationships.

At $E > 300$ mV the adsorption of oxygen species begins. The inset to Fig. 8 shows that in this region, the charge number changes sign and becomes positive. Consistently, Fig. 6 shows that the slope of the ΔG plot also changes sign in this range of potentials. The adsorption of hydrogen atoms may be neglected in this region. The charge number $l_{OH} < 0$ and hence charges flowing to the interface per OH_{ad} and per adsorbed chloride have the same sign. With the help of this information and Eq. (9) we can conclude that the sign inversion for the measured charge number l is caused by $\partial\Gamma_{OH}/\partial\Gamma_{Cl^-} < 0$. The negative sign of this derivative indicates that adsorption of chloride and the oxygen species has a competitive character.

Introducing the Parsons' function $\xi = \gamma + QE$ into Eq. (2) and cross-differentiating the expression for $d\xi$ yields the following expression for the Esin–Markov coefficient:

$$\frac{1}{RT}\left(\frac{\partial E}{\partial \ln c_{KCl}}\right)_Q = -\left(\frac{\partial\Gamma_{Cl^-}}{\partial Q}\right)_{\ln c_{KCl}} \quad (11)$$

Eq. (11) relates directly measured quantities such as E, Q and the bulk concentration of KCl to the Gibbs excess. The calculation involves one integration and one differentiation step. Therefore, Eq. (11) may be used to check that no major errors were made in the calculation of Γ_{Cl^-}. Fig. 9 shows Γ_{Cl^-} plotted versus ΔQ at constant bulk KCl concentration for the 'double layer' region of the Pt(111) electrode. The plots are

fairly linear, and their slopes give the Esin–Markov coefficients. The Esin–Markov coefficients can be calculated independently from the slope of E versus $RT \ln c_{KCl}$ plots at constant ΔQ shown in Fig. 10. The two independently determined derivatives are plotted against each other in Fig. 11. The points show the experimental data, and the dotted line is a line of unit slope. The experimental points scatter randomly around the dotted line indicating that the Γ_{Cl^-} data are free from major data-processing errors.

The reciprocal of the Esin–Markov coefficient gives the charge flowing to the interface per adsorbed Cl^- at constant bulk KCl concentration (n):

$$n = -\frac{1}{F}\left(\frac{\partial \Delta Q}{\partial \Gamma_{Cl^-}}\right)_{KCl} \quad (12)$$

For the 'double layer' region the values of n calculated from the Esin–Markov coefficients range from -0.9 to -1.15 in good agreement with the magnitude of the charge numbers at constant potential reported in the preceding section.

4. Conclusions

The chronocoulometric method and a thermodynamic analysis of the charge density data have been employed to study adsorption of chloride ion at the Pt(111) electrode surface. The results indicate that chloride ion forms a strong chemisorption bond with the platinum surface. The adsorption involves a significant redistribution of charge at the interface, and the polarity of the chemisorption bond is very small. Effectively, the adsorbed species can be considered as adsorbed chlorine atoms. Chloride adsorption at Pt is affected by the adsorption of hydrogen at negative potentials and by an oxygen species (OH_{ad}) at positive potentials. It has been demonstrated that adsorption of hydrogen and chloride is synergistic in character. In contrast, chloride and the OH_{ad} compete for sites at the surface.

Acknowledgements

This work was supported by a grant from Natural Sciences and Engineering Research Council of Canada.

References

[1] C.A. Lucas, N.M. Markovic, P.N. Ross, Phys. Rev. B 55 (1997) 7964.
[2] J.M. Orts, R. Gomez, J.M. Feliu, A. Aldaz, J. Clavilier, Electrochim. Acta 39 (1994) 1519.
[3] D.A. Stern, H. Baltruschat, M. Martinez, J.L Stickney, D. Song, S.K. Lewis, D.G. Frank, A.T. Hubbard, J. Electroanal. Chem. 217 (1987) 101.
[4] G.A. Garwood, Jr., A.T. Hubbard, Surf. Sci. 112 (1981) 281.
[5] R. Schennach, E. Bechtold, Surf. Sci. 380 (1997) 9.
[6] R. Schennach, E. Bechtold, Surf. Sci. 369 (1996) 277.
[7] B. Kloetzer, E. Bechtold, Surf. Sci. 326 (1997) 218.
[8] F. Wagner, T.E. Moyan, Surf. Sci. 216 (1989) 361.
[9] D.H. Fairbrother, J.G. Roberts, G.A. Somorjai, Surf. Sci. 399 (1998) 109.
[10] G. Horanyi, E.M. Rizmayer, J. Electroanal. Chem. 218 (1987) 337.
[11] B.I. Nodlovchenko, T.D. Gladysheva, O.V. Vyaznikovtseva, Yu.M. Volfkovich, Sov. Electrochem. 19 (1983) 381.
[12] D.M. Novak, B.E. Conway, J. Chem. Soc. Faraday Trans. 1 77 (1981) 2341.
[13] F.V. Molina, D. Posadas, Electrochim. Acta 33 (1988) 661.
[14] J. Weber, Y.B. Vasil'ev, V.S. Bagotskii, Sov. Electrochem. 5 (1969) 290.
[15] D.A. Rose, I. Benjamin, J. Chem. Phys. 98 (1993) 2283.
[16] D.M. Kolb, in: H. Gerischer, C. Tobias (Eds.), Advances in Electrochemistry and Electrochemical Engineering, vol. 11, Wiley, New York, 1978.
[17] R Michaelis, M.S. Zei, R.S. Zai, D.M. Kolb, J. Electroanal. Chem. 339 (1992) 299.
[18] N. Markovic, P.N. Ross, J. Electroanal. Chem. 330 (1992) 499.
[19] N.M. Markovic, H.A. Gasteiger, C.A. Lucas, I.M. Tidswell, P.N. Ross, Surf. Sci. 335 (1995) 91.
[20] I.M. Tidswell, C.A. Lucas, N.M. Markovic, P.N. Ross, Phys. Rev. B 51 (1995) 10205.
[21] C.A. Lucas, N.M. Markovic, I.M. Tidswell, P.N. Ross, Physica B 221 (1996) 245.
[22] H.S. Yee, H.D. Abruna, J. Phys. Chem. 97 (1993) 6278.
[23] R. Gomez, H.S. Yee, G.M. Bomminarito, J.M. Feliu, H.D. Abruna, Surf. Sci. 355 (1995) 101.
[24] B.C. Schardt, J.L. Stickney, D.A. Stern, A. Wieckowski, D.C. Zapien, A.T. Hubbard, Surf. Sci. 175 (1986) 520.
[25] D.R. Wheeler, J.X. Wang, R.R. Adzic, J. Electroanal. Chem. 387 (1995) 115.
[26] C. Wang, C.-S. Chung, S.-C. Chan, J. Electroanal. Chem. 395 (1995) 317.
[27] W. Savich, S.G. Sun, J. Lipkowski, A. Wieckowski, J. Electroanal. Chem. 388 (1994) 347.
[28] J. Clavilier, D. Armand, S.-G. Sun, M. Petit, J. Electroanal. Chem. 205 (1986) 267.
[29] J. Richer, J. Lipkowski, J. Electrochem. Soc. 133 (1986) 121.
[30] A.N. Frumkin, O.A. Petrii, Electrochim. Acta 20 (1975) 347.
[31] R. Parsons, Trans. Faraday Soc. 51 (1955) 1518.
[32] G. Valette, A. Hamelin, R. Parsons, Z. Phys. Chem. Neue Folge 113 (1978) 71.
[33] K. Bange, S. Strachler, J.K. Sass, R. Parsons, J. Electroanal. Chem. 205 (1987) 87.
[34] W. Schmickler, R. Guidelli, J. Electroanal. Chem. 235 (1987) 387.